

Anti-counterfeit nanoscale fingerprints based on randomly distributed nanowires

Jangbae Kim¹, Je Moon Yun¹, Jongwook Jung¹, Hyunjoon Song^{1,2}, Jin-Baek Kim¹ and Hyotcherl Ihee^{1,2}

¹ Department of Chemistry, Korea Advanced Institute of Science and Technology (KAIST), Daejeon 305-701, Republic of Korea

² Center for Nanomaterials and Chemical Reactions, Institute for Basic Science (IBS), Daejeon 305-701, Republic of Korea

E-mail: hyotcherl.ihee@kaist.ac.kr

Received 21 December 2013, revised 29 January 2014

Accepted for publication 13 February 2014

Published 20 March 2014

Abstract

Counterfeiting is conducted in almost every industry, and the losses caused by it are growing as today's world trade continues to increase. In an attempt to provide an efficient method to fight such counterfeiting, we herein demonstrate anti-counterfeit nanoscale fingerprints generated by randomly distributed nanowires. Specifically, we prepare silver nanowires coated with fluorescent dyes and cast them onto the surface of transparent PET film. The resulting non-repeatable patterns characterized by the random location of the nanowires and their fluorescent colors provide unique barcodes suitable for anti-counterfeit purposes. Counterfeiting such a fingerprint pattern is impractical and expensive; the cost of replicating it would be higher than the value of the typical target item being protected. Fingerprint patterns can be visually authenticated in a simple and straightforward manner by using an optical microscope. The concept of generating unique patterns by randomness is not limited to the materials shown in this paper and should be readily applicable to other types of materials.

Keywords: anti-counterfeit, fingerprint, fluorescence, nanowire, randomness

 Online supplementary data available from stacks.iop.org/Nano/25/155303/mmedia

1. Introduction

Counterfeiting is a steadily increasing and important problem that affects all types of commercialized production. According to the World Customs Organization, ~6% of global goods traded are counterfeit. The sale of counterfeit goods occurs in nearly every trade and industry affecting our daily life because of globalization and the growth of internet trade. In many cases, it is very difficult to distinguish counterfeit goods from genuine products. Ironically, to some extent, customer demand encourages the counterfeiting business.

To date, there have been numerous attempts at anti-counterfeiting, including holography [1–3], laser surface authentication (LSATM) [4], radio frequency identification (RFID) [5], nano barcodes [6, 7], surface enhanced Raman

scattering (SERS) and quantum dot tags [8, 9], and nanocomposite tags [10]. In this paper, we propose a new approach based on fingerprint patterns generated by randomly distributed nanorods. Our key idea is that a unique pattern is generated simply by casting a handful of nanorods onto a plate. Because of naturally occurring randomness, the probability of obtaining identical patterns is practically zero. Therefore, each pattern generated by simple casting is unique, like a fingerprint, and can thus be used as a security code or barcode. If we expand this concept further, we can find some nano or subnano (or even micro and above) scale defects on the surfaces of many products, such as paper documents, whose defect profiles can also be recorded as unique barcodes. However, it would be more beneficial to create unique patterns on the location selected for identification. For this purpose,

we prepared a fingerprint pattern on a transferable film, specifically a flexible polyethylene terephthalate (PET) film, on which direction and target markers were patterned by a photolithographic technique to provide positional information for identification. The target marker has a specified observation region in which a hidden fingerprint pattern is prepared using randomly distributed silver nanowires (AgNWs). A simple, low-magnification optical microscope can be used to verify the fingerprint pattern. The complexity of the pattern can be further increased by coating the surfaces of the AgNWs with fluorescent dyes of various colors (red and green in this work); in this case, verification can be achieved by a fluorescence microscope. This fingerprint patterning technique is easily transferable to any surface and provides artificial fingerprints as nanoscale stamps. The authenticity verification is simple and straightforward, allowing customers to immediately determine whether products are authentic. Our technique is sufficiently simple that anyone can prepare fingerprint patterns that cannot be reproduced as a result of the underlying basic principle of randomness. This naturally occurring event enabled us to prepare novel fingerprint labels that can be used to combat potential counterfeiting attempts.

2. Materials and methods

2.1. Synthesis of AgNWs

A 3.0 ml solution of PVP (0.6 M, M.W. 55 000, Sigma-Aldrich, Missouri, USA) and a 3.0 ml solution of AgNO₃ (0.10 M, 99.999%, Sigma-Aldrich, Missouri, USA) in ethylene glycol (Sigma-Aldrich, Missouri, USA) were alternately added to 5.0 ml of boiling ethylene glycol every 30 s over a 7.5 min period. The resulting mixture was refluxed at ~160 °C for 1 h. The final solution was cooled, and the small particles were removed by centrifugation at 1500 rpm for 10 min. The product was purified by repetitive dispersion and precipitation cycles with ethanol (Junsei, Japan) to remove excess PVP and then dispersed in ethanol (40 ml).

2.2. Silica coating of the AgNWs

A total of 0.350 ml of aqueous 30 vol.% NH₄OH (Junsei, Japan) was mixed with 9.09 ml of isopropyl alcohol (Junsei, Japan), and 0.11 ml of tetraethyl orthosilicate (TEOS) (Sigma-Aldrich, Missouri, USA) was mixed with 7.9 ml of isopropyl alcohol. A total of 2.00 ml of DI-H₂O was first added to 5.0 ml of the AgNW dispersion, followed by the dropwise addition of the isopropyl alcohol solution of NH₄OH. After 30 s, the isopropyl alcohol solution of TEOS was added to the final AgNW dispersion. The final solution was stirred for 40 min to form silica-coated AgNWs.

2.3. FITC- or RITC-doped silica coating of the AgNWs

FITC (fluorescein isothiocyanate, Sigma-Aldrich, Missouri, USA) and RITC (rhodamine B-isothiocyanate, Sigma-Aldrich, Missouri, USA) were covalently linked to 3-aminopropyl trimethoxysilane (APTMS, TCI, Japan) by dissolving 100 mg of FITC in 186 μl of APTMS and 100 mg of RITC in 135 μl

of APTMS. Then, ethanol was added to make a 10 vol.% dye-linked APTMS in ethanol solution. The ethanol solution of dye-linked APTMS was stirred for 24 h in the dark prior to use. The silica-coated AgNW dispersion (1 ml) was added dropwise to 0.4 ml of isopropyl alcohol under vigorous stirring, followed by the addition of 0.1 ml DI-H₂O. Separately, 0.126 ml of the NH₄OH was mixed with 9.62 ml of isopropyl alcohol, and 0.1 ml of ethanol solution of the dye-linked APTMS was mixed with 9.9 ml of isopropyl alcohol. Next, 0.72 ml of the isopropyl alcohol solution of NH₄OH was added dropwise to the AgNW dispersion. After 30 s, 0.2 ml of the alcoholic solution of dye-linked APTMS was added to the AgNW dispersion. The final solution was stirred for 24 h.

2.4. Preparation of the photolithographic pattern on PET

A PET film was cut into strips 3 cm × 3 cm in size. The PET strips were ultrasonically cleaned for 5 min in acetone, followed by chloroform. A negative-tone SU-8 2000.5 (0.25 mg ml⁻¹, MicroChem Corp., Massachusetts, USA) photoresist incorporating fluorescent dye (RB) was dropped onto the cleaned PET strips. The initial spin was set at 500 rpm for a period of 10 s to spread the photoresist over the entire sample surface and then at 2000 rpm for 50 s. The coated samples were then soft baked on a hotplate at 95 °C for 90 s to remove organic solvent. After the baking process, to prepare direction and target marker pattern arrays, the samples were exposed to UV light through a photomask with the appropriate design features for 45 s using a collimated UV source (13.1 mW cm⁻², MDA-6000DUV, MAIDAS System Co, Korea). A post-exposure baking process was performed on a hotplate at 95 °C for 5 min. Afterward, the samples were developed in SU-8 developer for 60 s, rinsed with 2-propanol, and dried in a stream of nitrogen.

2.5. Preparation of the fingerprint pattern on PET

The preparation of the fingerprint pattern simply involved alternately dropping a predetermined amount of FITC- or RITC-coated AgNW dispersion onto the target marker. Alternatively, the dye-coated AgNW dispersion was premixed in any ratio, and this solution was dropped onto the target marker. Simply increasing the amount of solution dropped could increase the number density of dye-coated AgNWs in the observation region. In addition, various mixing ratios between the two colors of the dye-coated AgNW dispersion could generate numerous different subset patterns. Practically, 1 μl of solution was more than sufficient for the preparation of five or six fingerprint patterns.

2.6. Fluorescence microscopy

The optical and fluorescence images of the dye-labeled fingerprinting patterns were observed using an inverted fluorescence microscope (IX71, Olympus) equipped with filter set types U-MWB2 (460–490 nm excitation and 500 nm dichromatic mirror) and U-MWG2 (510–550 nm excitation and 570 nm dichromatic mirror). Direct visualization of the fingerprinting pattern was achieved via excitation of the FITC/RITC-labeled

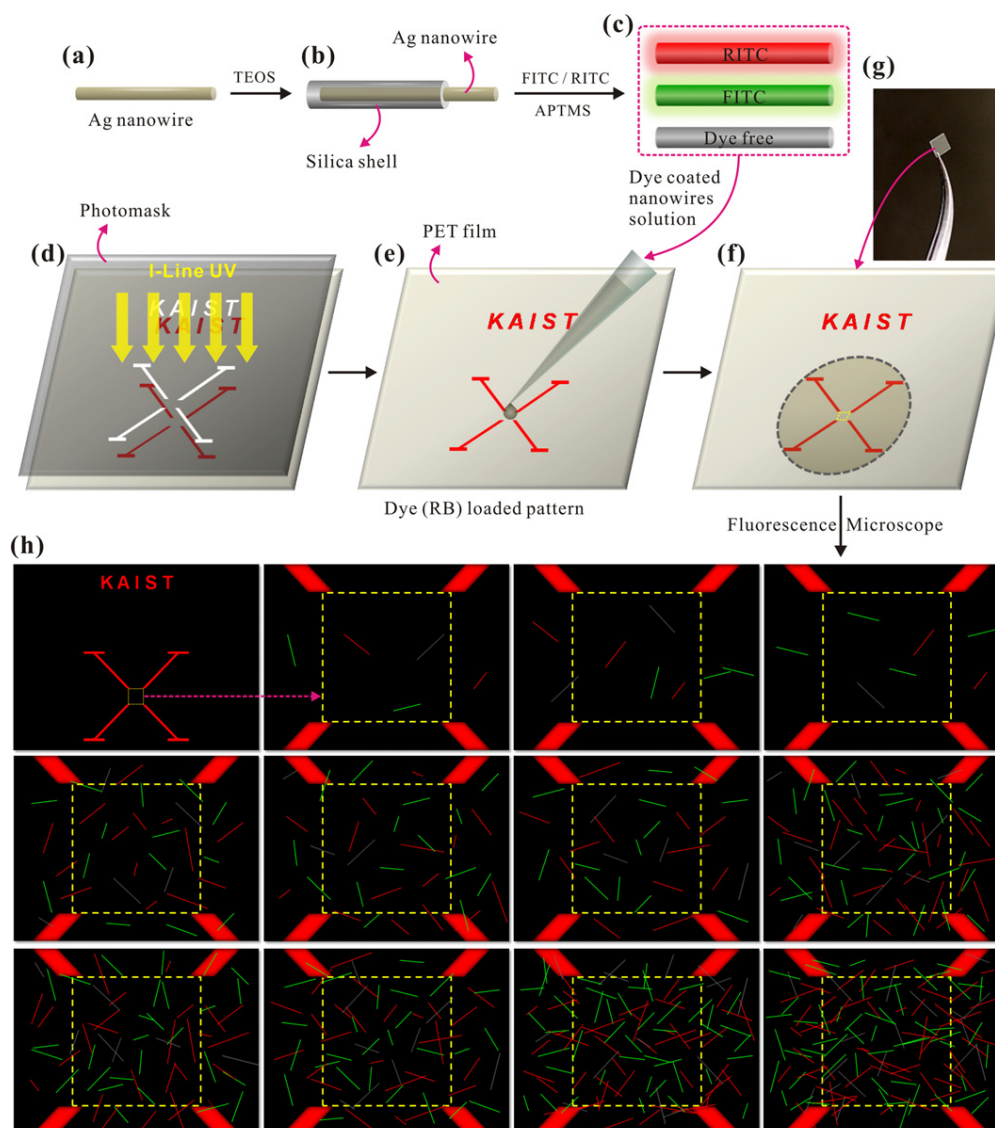


Figure 1. A schematic for anti-counterfeit nano-fingerprints based on randomness. We used Ag nanowires (AgNWs) to create fingerprint patterns on the surface of a PET film. (a) A AgNW with a diameter of ca. 70 nm prepared by the self-seeding method. (b) Coating an amorphous silica shell on the surface of the AgNW by using tetraethyl orthosilicate (TEOS). (c) Preparation of fluorescent-dye-coated AgNWs. Fluorescein isothiocyanate (FITC) and rhodamine B-isothiocyanate (RITC) are attached covalently to the surface of the pre-formed silica shell by allowing the formation of covalent bonds between the silica surface and 3-aminopropyltrimethoxysilane (APTMS). (d) The photolithographic process used to inscribe the direction and target markers on the surface of the PET film. The orientation marker ('KAIST') can be used to determine the correct direction of the PET film. The target marker ('X') has an empty space in its central region where AgNWs are loaded to generate fingerprints. (e) Preparation of a fingerprint pattern on the surface of the target marker by dropping a solution of AgNWs coated with fluorescent dyes. (f) A fingerprint pattern is generated in the central region of the target marker (yellow dotted rectangle) upon evaporation of the solvent. (g) Flexible transparent PET film (thickness 100 μm , 5 mm \times 5 mm) with a covert fingerprint pattern. (h) Schematic illustration of typical fingerprint patterns (indicated by yellow dotted rectangles) in the central region of the target marker on the surface of PET. The complexity of the pattern can be easily increased by increasing the number density of nanowires.

nanowires and rhodamine B-doped photolithographic pattern using a UV-mercury lamp (100 W). The illuminated light was directed through a U-MWB2 or U-MWG2 filter for green or red excitation, respectively.

2.7. Scanning and transmission electron microscopy

The prepared AgNWs were analyzed by a field-emission scanning electron microscope (FE-SEM, Hitachi S-4800, Japan). Samples for TEM examination were prepared by transferring

the silver nanowire solution onto copper grids and drying under ambient conditions. High-resolution TEM observation was performed on a Tecnai F20 (Philips) field-emission transmission electron microscope (FE-TEM) at an acceleration voltage of 200 kV.

3. Results and discussion

Figure 1 schematically depicts the preparation and identification of covert fingerprint patterns on the surface of PET

film. AgNWs were chosen as the basic materials for random patterns because (1) they can be easily observed by optical or fluorescence microscopy, (2) their anisotropic well-defined 1D structure is suitable for generating unique patterns, and (3) they can be prepared routinely in high volume by a facile process [11–13]. In principle, however, any NW or nanoscale (or even any) object can be used (figure 1(a)). We prepared AgNWs via the self-seeding process according to the literature [12, 13]. The resulting AgNWs had an average length of 10–50 μm and an average diameter of 70 ± 6 nm (figure S1 available at stacks.iop.org/Nano/25/155303/mmedia). The AgNW dispersion in ethanol usually contains a small amount of nanoparticles, even after centrifugation. Although they make the overall pattern appear noisier, these nanoparticles actually increase the complexity of the pattern.

While the AgNW-based random patterns alone served our purpose, we added complexity by coloring the AgNWs with various fluorescent dyes so that the hidden color information could be detected only via fluorescent detection. To achieve this goal, we formed amorphous silica shells on the surfaces of the as-synthesized AgNWs by employing a previously reported method [14, 15]. The prepared silica layer was further reacted with fluorescent dyes (fluorescein isothiocyanate, FITC; rhodamine B-isothiocyanate, RITC) linked to 3-aminopropyltrimethoxysilane (APTMS) to prepare dye-coated AgNWs by allowing the formation of covalent bonds between the silica surface and the APTMS (figures 1(b) and (c)). The silica layer not only provides the surface chemistry necessary to attach fluorescent dyes to its surface covalently but also enhances visibility by increasing the thickness of the AgNW (ca. 212 nm). Considering the resolution limit of the optical microscope, thickness increase is highly preferable. With green light (550 nm), the estimated optical resolution limit is approximately 350 nm. In practice, the lowest value obtainable with conventional lenses is approximately 200 nm [16]. Note that fluorescent dyes should be attached to the surface of a pre-formed silica shell to avoid the dissolution of core AgNWs, which occurs if the silica coating and fluorescent dye coating are performed simultaneously. A small portion of AgNWs were found to remain intact, even after the fluorescent dye molecules were conjugated to the silica layer. These non-fluorescent AgNWs were also used as basic components for generating the fingerprint pattern because they could not be removed from the fluorescent AgNW mixture. The randomly distributed fingerprint pattern became increasingly complex as a result of the existence of non-fluorescent AgNWs because all optically active AgNWs under bright field observation do not contribute to the fluorescent images.

A flexible transparent PET film was used as the substrate on which a rhodamine B (RB) dye-incorporated photoresist (SU-8 2000.5) pattern was prepared by a conventional photolithographic technique using an I-Line UV (figure 1(d)). After the photolithographic processes had been performed, the orientation marker ('KAIST') and the target marker ('X') were prepared on the surface of the flexible PET film. The thickness of the prepared markers was measured to be ca. 600 nm from the flat surface. The orientation marker indicates

the correct observation direction for the flexible PET film. That is, the correct orientation of the PET film is defined as the directional placement in which we can read the label 'KAIST' correctly (figure S2 available at stacks.iop.org/Nano/25/155303/mmedia). The target marker ('X') in the center of the PET film indicates the location of the observation region, which has dimensions of $100 \mu\text{m} \times 100 \mu\text{m}$ (figure 1(e)), where the randomly distributed fluorescent-dye-coated AgNWs are cast, and thereafter the fingerprint patterns can be observed using an optical or fluorescence microscope. Because the letter 'X' has dimensions of $800 \mu\text{m} \times 700 \mu\text{m}$, with a line width of $20 \mu\text{m}$ and a height of ca. 600 nm, the existence of prepared patterns can be identified even by the naked eye. Once we have confirmed the ideal position of the substrate using the orientation marker, the target marker can be easily observed by moving down from the orientation marker by $590 \mu\text{m}$, and the observation region can consequently be readily identified by following the lines of the 'X'.

The fingerprint patterns are prepared by dropping a predetermined amount of AgNW dispersion on the target marker on the surface of the PET film, followed by air drying (figure 1(e)). Upon solvent evaporation, a random distribution of the dye-coated AgNWs on the film occurs, thereby leading to the formation of a unique fingerprint pattern (figure 1(f)). Notably, a flexible transparent PET film with a thickness of $100 \mu\text{m}$ presents advantages with respect to application and processing. One of the greatest advantages of such a PET film is that it can be cut to any size and shape and attached to various surfaces via simple treatments (figure 1(g)).

The prepared fingerprint pattern can be easily observed by using an optical/fluorescence microscope, as represented schematically in figure 1(h). As mentioned previously, we can identify the correct orientation using the orientation marker ('KAIST'), which in turn allows us to easily find the target marker ('X'). Based on magnified ($1000\times$) images focusing on the observation region in the center of the target marker (yellow dotted square), the fingerprint pattern can be readily identified. Thereafter, these observed fingerprint images can be stored in a database with intrinsic ID numbers for authenticity verification. The number of AgNWs distributed in the observation region can be easily controlled by the concentration of fluorescent AgNWs. Various schematic fingerprint patterns are represented by the number density of nanowires and the distribution patterns in figure 1(h). Considering the large number of cases that can be generated by distributing a single AgNW in a square measuring $100 \mu\text{m} \times 100 \mu\text{m}$, several tens of AgNWs can generate a nearly infinite number of unique distribution patterns, for which the probability of obtaining two identical patterns is practically zero.

We prepared many fingerprints on the surface of PET film and selected 12 sets for clear visualization, as shown in figure 2. Figure 2(c) represents the fingerprint patterns with enhanced visibility that were created by employing fluorescent-dye-coated AgNWs with an average diameter of ca. 392 nm, which is 1.8 times thicker than the AgNWs in figures 2(a) and (b). All of the observed images from the PET film (figure 2) show distinct, randomly distributed patterns, and no identical images can be found. Here, three major factors

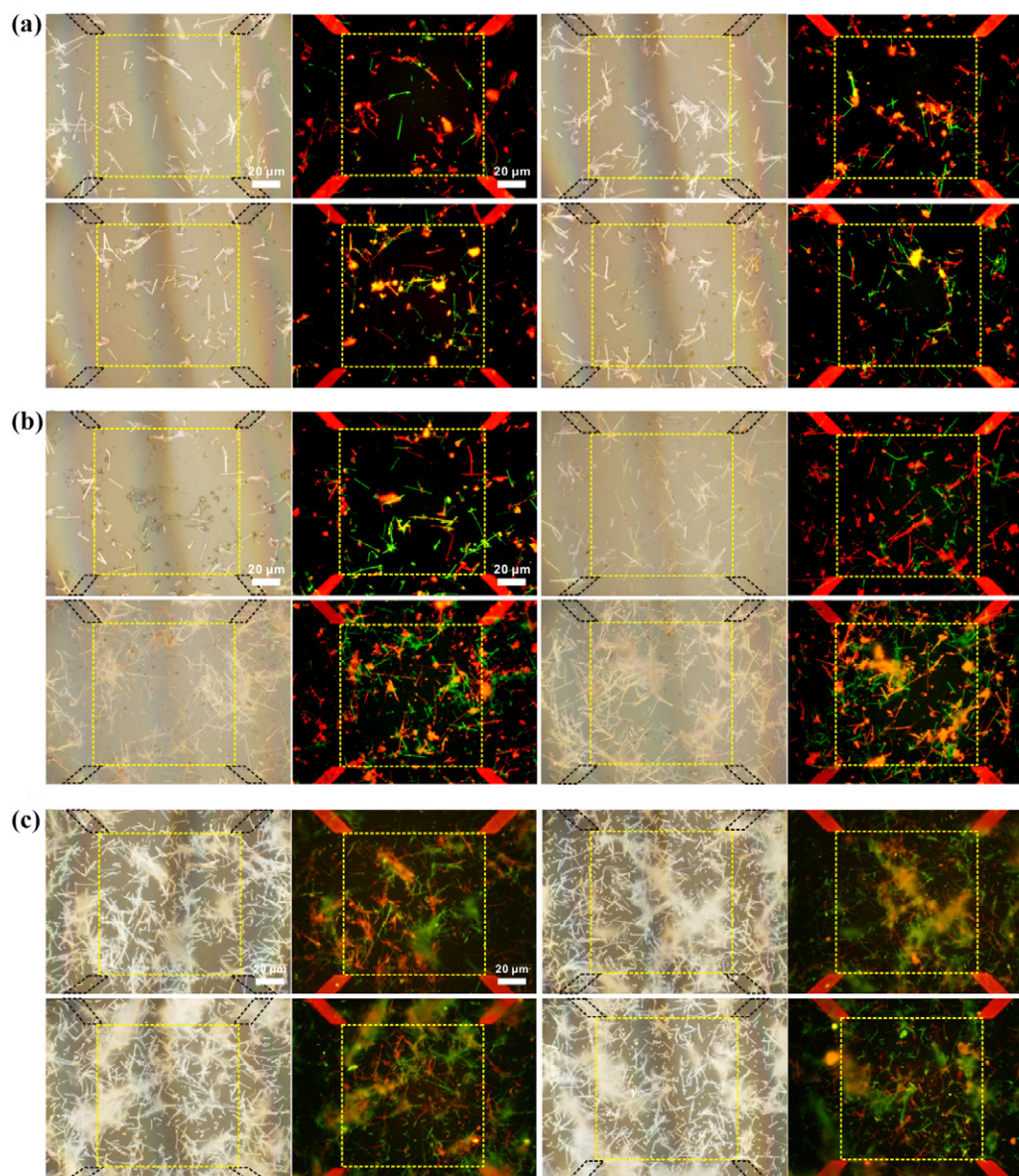


Figure 2. A series of fingerprint patterns with various number densities of dye-coated AgNWs. A series of bright field optical (left) and fluorescence (right) images are displayed with target markers (black dotted parallelograms) and central fingerprint regions (yellow dotted rectangles; $100\ \mu\text{m} \times 100\ \mu\text{m}$) for better visualization for three number densities of AgNWs: (a) low, (b) medium and (c) high. The fluorescence images are prepared by combining individual red and green fluorescence images that are detected from the same viewpoint and field of interest. The scale bar shown in the first figure is common for all figures. The average diameters of the AgNWs are ca. 200 nm, ca. 212 nm, and 392 nm for (a), (b), and (c), respectively.

govern the generation of fingerprints: (1) the lack of AgNWs with identical lengths in the observation region, (2) nearly infinite spatial (position and orientation) degrees of freedom generated by multiple AgNWs inside the observation region, and (3) varied mixing ratios between the two different colors as well as fluorescently inactive objects. Thus, the combination of these factors makes the number of cases for potential random patterns practically infinite. Furthermore, the nanoparticles that remain in the AgNW dispersion also contribute to the complexity of the fingerprint pattern (figure 2).

As a final step, a unique ID (barcode) can be assigned to each unique fingerprint; this ID can facilitate a quick search in a database. The authentication process would be the same as the

pattern observation process using a microscope (figure 1(h)). If the substrate is positioned in the correct orientation, the bright field and fluorescence images of the observation region can be displayed and visually compared with the stored images. Comparison of both bright field and fluorescent images will minimize the occurrence of authentication failures as a result of non-fluorescent AgNWs. These authentication processes can be automated by employing an algorithm that recognizes the positions and colors of the AgNWs and digitizing that information in a database. Such digitized information could significantly reduce the size of the stored data and reduce the time required for the authentication process.

For practical applications, one needs to consider the effect of the particles on image quality and the durability of the fingerprint pattern including stability of fluorescence and protection against external perturbation. The presence of the particles not only has an advantage in increasing the complexity of the pattern but also has a drawback in terms of the image quality. Since the pattern recognition process has to involve image recording and processing by a camera under optical microscopy, the presence of Ag particles may make it hard to acquire high fidelity images (especially for high-density particles/wires observed under dark field mode). This could lead to undesirable difficulties in image recording and processing. To resolve this issue, a separation technique [17] that can remove most particles from the wires would be useful.

The number of cases for distributing 0D isotropic dots and 1D anisotropic NWs in a rectangular area can be calculated by employing the following simple model. First, the number of cases for distributing 0D dots in a rectangular area is given by $N = SC_P$, where S is the number of sites and P is the number of dots. For NWs, an additional factor needs to be added to account for the rotational degree of freedom coming from the 1D nature of the NWs. For most NWs except those whose ends are very near the edge of the observation window, the rotational degrees of freedom can be defined by $360/n$, where n is the smallest rotation angle that can be resolved with the resolution of a typical optical microscope. Thus, the number of cases for NWs can be approximated as $SC_P \times (360/n)^P$. Here, for simplicity, we consider only the case where at least one end of the NW is within the observation area and the length of the NW is considerably smaller than the size of the observation area. Due to this simplification, the length of the NW is not in the equation. The lower bound for the number of sites can be approximated by dividing the total area of observation by the projection area of the object (0D dot or 1D NW), which is roughly the square of the diameter of the 0D dot or the square of the width of the 1D NW, provided that the diameter or the width is larger than the spatial resolution allowed by the optical microscope. Otherwise, the spatial resolution of the microscope can be used as the practical diameter or width for estimating the number of sites. If the objects are coated with three different colors to increase randomness, an additional factor of 3^P needs to be added, giving $SC_P \times 3^P$ for 0D dots and $SC_P \times (360/n)^P \times 3^P$ for 1D NWs. These numbers are given when the size or the length of the objects used is known. In reality, such sizes may not be easily predictable, and thus these numbers give only the lower bounds for the practical number of cases. Furthermore, the objects are not truly identical because the diameters and lengths of the NWs vary. Based on these facts, the number of cases for distributing 1D NWs approaches infinity. As a simple scenario, we can consider the case for using only a single object. For simplicity, we consider a 0D dot with a diameter of 500 nm or a 1D NW with a width of 500 nm and a length of 10 μm and assume that the microscope can resolve 500 nm. For an observation area of 100 μm by 100 μm , S can be approximated as 40 000 ($= (100 \times 100) / (0.5 \times 0.5)$). In this case, the number of cases for distributing a single 0D dot ($P = 1$) in the rectangular area

is simply 40 000 ($= 40\,000C_1$). If we employ three colors for each object, the calculated number of cases for the 0D dot is 120 000 ($= 40\,000C_1 \times 3^1$). For the 1D NW, the orientation factor, $(360/n)^P$, needs to be further added. If we assume that the microscope can discriminate the orientation with a resolution of 10° , which is quite a conservative value, then the effective orientation factor is 36 ($= (360/10)^1$), giving a total number of cases of 4 320 000 ($= 40\,000C_1 \times 3^1 \times (360/10)^1$) for the 1D NW. When two objects are employed for generating random patterns ($P = 2$), the number of cases for two 0D dots is 7199 820 000 ($= 40\,000C_2 \times 3^2$) and that for two NWs is 9330 966 720 000 ($= 40\,000C_2 \times 3^2 \times (360/10)^2$). Just four NWs can make the number of cases comparable to Avogadro's number. In this regard, it may not be helpful to have too many wires for practical applications that require the pattern to be easily recorded by the manufacturer and recognized by users because wire overlap may obscure the pattern recognition process. On the other hand, if the number of objects is too small, mimicking of the pattern would be possible. Thus, for practical applications, the number of objects should be determined by considering the balance between efficiency of image processing which favors a small number of objects and difficulty of counterfeiting which favors a large number of objects.

Because the AgNW-based fingerprints generate random patterns and an individual AgNW cannot be easily manipulated because of the nanoscale size, it is nearly impossible to replicate the fingerprint patterns via artificial manipulation as long as the number of objects is not too small. Moreover, the cost of generating such an identical counterfeit pattern would generally be much higher than the value of the typical product being protected. This factor and the simple preparation of fingerprint patterns and authenticity verification are attractive advantages of this technique. Specifically, authenticity verification can be performed by general customers. Furthermore, this technique can be applied directly to numerous products, including paper and credit cards, without using conventional substrates or photoresist patterns.

An important issue concerning the practical application of fluorescent-dye-coated nanowires is storage life and the stability of fluorescence over time. In a previous report, the fluorescence stability and storage life of FITC-labeled bead arrays was measured [18]. The samples were stored in the dark at 4°C over a period of two years, and measurements were performed every year with identical settings of the flow cytometer. The results showed that the measured fluorescence intensity decreased slightly after two years. The fractions in the histograms were still as distinguishable as before except for a slight peak shift along the fluorescence scale. Based on the result, we can expect that the storage life of FITC could be extended up to at least 2 years. In this regard, it may be more favorable to employ organic fluorescent wires [19] or use the optical reflectance of metal wires [20] to improve the durability of fingerprint patterns. On the other hand, it should be noted that the use of fluorescence is not essential for applications because the pattern is still useful, even after the fluorescence is lost.

The NWs can adhere to the substrate through various interactions or by their combination, such as through van der

Waals, hydrophobic, hydrophilic and electrostatic interactions. These interactions may not be strong enough to firmly protect the NWs on a substrate against external perturbation. As an approach to firmly fix the NWs on a substrate, a highly transparent and thin polymer film could be used to cover the entire random pattern. It is expected that the polymer film would be able to maintain the prepared random pattern in an observation region and protect it against external chemical or mechanical perturbation without the loss of image quality.

4. Conclusion

In this work, we prepared anti-counterfeit nanoscale fingerprints based on natural randomness by distributing fluorescent-dye-coated AgNWs on a PET film. A 1D NW can generate a larger number of cases than a 0D dot due to additional rotational degrees of freedom, and the introduced fluorescent dyes increase the complexity of the pattern. Simple mathematics shows that just four NWs can create a number of cases comparable to Avogadro's number without considering correlation parameters. This allows us to generate non-repeatable unique barcodes suitable for anti-counterfeit purposes. The most attractive advantages of this technique are the simple preparation of fingerprint patterns and authenticity verification. Fingerprint patterns can be visually authenticated in a simple and straightforward manner by using an optical microscope. Although generation of a fingerprint pattern is quite simple, counterfeiting of the pattern is essentially impossible because it is based on natural randomness. Even if it were possible to counterfeit the pattern, the cost of replicating it would be higher than the value of the typical target item being protected. Hence, we believe that this technique may significantly facilitate the identification of counterfeit goods and reduce counterfeiting activities.

Acknowledgment

This work was supported by the Institute for Basic Science (IBS) (CA1301-01).

References

- [1] Martinez C, Lemonnier O, Laulagnet F, Fargeix A, Tissot F and Armand M F 2012 Complementary computer generated holography for aesthetic watermarking *Opt. Express* **20** 5547–56
- [2] Wachulak P W, Bartels R A, Marconi M C, Menoni C S, Rocca J J, Lu Y and Parkinson B 2006 Sub 400 nm spatial resolution extreme ultraviolet holography with a table top laser *Opt. Express* **14** 9636–42
- [3] Wachulak P W, Marconi M C, Bartels R A, Menoni C S and Rocca J J 2007 Volume extreme ultraviolet nano-holographic imaging with numerical optical sectioning *Opt. Express* **15** 10622–8
- [4] Buchanan J D R, Cowburn R P, Jausovec A V, Petit D, Seem P, Xiong G, Atkinson D, Fenton K, Allwood D A and Bryan M T 2005 Forgery: 'fingerprinting' documents and packaging *Nature* **436** 475
- [5] Roberts C M 2006 Radio frequency identification (RFID) *Comput. Secur.* **25** 18–26
- [6] Penn S G, Norton S M, Walton I D, Freeman R G and Davis G 2004 Nanobarcodes particles as covert security tags for documents and product security *Proc. SPIE* **5310** 337–40
- [7] Demirok U K, Burdick J and Wang J 2009 Orthogonal multi-readout identification of alloy nanowire barcodes *J. Am. Chem. Soc.* **131** 22–3
- [8] Sun L-W, Shi H-Q, Li W-N, Xiao H-M, Fu S-Y, Cao X-Z and Li Z-X 2012 Lanthanum-doped ZnO quantum dots with greatly enhanced fluorescent quantum yield *J. Mater. Chem.* **22** 8221–7
- [9] Lu Z, Liu Y, Hu W, Lou X W and Li C M 2011 Rewritable multicolor fluorescent patterns for multistate memory devices with high data storage capacity *Chem. Commun.* **47** 9609–11
- [10] Johansen S, Radziwon M, Tavares L and Rubahn H G 2012 Nanotag luminescent fingerprint anti-counterfeiting technology *Nanoscale Res. Lett.* **7** 262
- [11] Korte K E, Skrabalak S E and Xia Y 2008 Rapid synthesis of silver nanowires through a CuCl- or CuCl₂-mediated polyol process *J. Mater. Chem.* **18** 437–41
- [12] Sun Y G, Gates B, Mayers B and Xia Y N 2002 Crystalline silver nanowires by soft solution processing *Nano Lett.* **2** 165–8
- [13] Sun Y G and Xia Y N 2002 Large-scale synthesis of uniform silver nanowires through a soft, self-seeding, polyol process *Adv. Mater.* **14** 833–7
- [14] Heitsch A T, Smith D K, Patel R N, Ress D and Korgel B A 2008 Multifunctional particles: magnetic nanocrystals and gold nanorods coated with fluorescent dye-doped silica shells *J. Solid State Chem.* **181** 1590–9
- [15] Yin Y D, Lu Y, Sun Y G and Xia Y N 2002 Silver nanowires can be directly coated with amorphous silica to generate well-controlled coaxial nanocables of silver/silica *Nano Lett.* **2** 427–30
- [16] Pedrotti L, Pedrotti L S and Pedrotti L M 2007 *Introduction to Optics* (Upper Saddle River, NJ: Prentice Hall)
- [17] Pradel K C, Sohn K and Huang J 2011 Cross-flow purification of nanowires *Angew. Chem. Int. Edn* **50** 3412–6
- [18] Schnäckel A, Hiller S, Reibetanz U and Donath E 2007 Fluorescent bead arrays by means of layer-by-layer polyelectrolyte adsorption *Soft Matter* **3** 200–6
- [19] Zheng J Y, Yan Y, Wang X, Zhao Y S, Huang J and Yao J 2012 Wire-on-wire growth of fluorescent organic heterojunctions *J. Am. Chem. Soc.* **134** 2880–3
- [20] Nicewarner-Pena S R, Freeman R G, Reiss B D, He L, Pena D J, Walton I D, Cromer R, Keating C D and Natan M J 2001 Submicrometer metallic barcodes *Science* **294** 137–41